

---

# Fractional active robust control

## Control of lightly-damped plants using the isodamping contours and the CRONE approach

**Valérie Pommier-Budinger \*** - **Yaman Janat\*** -  
**Dominique Nelson-Gruel\*\*** - **Patrick Lanusse\*\*** - **Alain Oustaloup\*\***

\* *Université de Toulouse – ISAE*  
10, avenue E. Belin, BP 54032, F-31055 Toulouse - France  
valerie.budinger@isae.fr

\*\* *IMS/LAPS UMR 5218 CNRS/Université de Bordeaux*  
351, cours de la Libération, F-33405 Talence, France

---

*RESUME.* Cet article concerne le contrôle de vibrations. Ce problème peut être résolu par des méthodes passives avec des systèmes amortissant ou bien par des méthodes actives avec des actionneurs contrôlés pour diminuer voire annuler complètement les vibrations dans la structure. La seconde méthode est employée dans les travaux décrits dans cet article. L'objectif précis est de contrôler l'amortissement de systèmes peu amortis et incertains. La méthode proposée met en œuvre les contours d'isoamortissement et la commande CRONE. Les contours d'isoamortissement sont définis dans le plan de Nichols grâce à l'intégration d'ordre non entier et sont gradués par le coefficient d'amortissement de la réponse en boucle fermée. La commande CRONE est une méthode de contrôle robuste basée sur l'intégration d'ordre non entier également. La méthode est ici appliquée à un procédé multivariable qui est une maquette d'aile d'avion composé d'une poutre encastree-libre avec un réservoir dont les différents niveaux de remplissage sont considérés comme des incertitudes.

*KEYWORDS:* Commande robuste d'ordre non entier multivariable; contrôle actif, contours d'iso-amortissement.

---

*ABSTRACT.* This article deals with the reduction of structural vibrations. Two approaches are possible to tackle this problem, either a passive method with dampers, or an active method with actuators that are controlled in order to decrease or even cancel the vibrations in the structure. The second method is used here. The objective is to control the damping of uncertain plants. The proposed methodology is based on iso-damping contours and CRONE control. The iso-damping contours are defined thanks to fractional order integration in the Nichols plane and are graduated by the value of the damping factor of the closed-loop response. The CRONE control is a robust control method that also uses fractional order integration. The methodology is here applied to a multivariable plant that is an aircraft wing model made with a beam and a tank whose different levels of fillings are considered as uncertainties.

*KEYWORDS:* fractional order multivariable control; active control; robust control; iso-damping contour.

---

## 1. Introduction

The reduction of structural vibration has been challenging engineers for many years. Innumerable applications exist where vibration control is beneficial, if not essential. In the control of vibrations, the damping factor is an important data since it indicates how quickly the vibrations decrease. When control of vibrations is at stake, it can be useful to control this parameter. Works have already been achieved to this end (Yq and Moore, 2005).

This article proposes a method in the frequency-domain to control uncertain plants while ensuring the damping factor of the response. This method is based on the complex fractional order integration (Samko *et al.*, 1993; Miller and Ross, 1993) that makes it possible to define an open-loop transfer function whose Nichols locus is an any-direction straight line segment called “generalized template”. This transfer function is used:

- for the construction, in the Nichols plane, of the “iso-damping” contours whose graduation is the damping factor (Oustaloup *et al.*, 1995),
- for the CRONE control methodology applied in this article (Oustaloup *et al.*, 1999a).

The article falls into 6 parts. Section 2 introduces the transfer function of a complex non-integer integrator defining a generalized template which will be considered as part of an open-loop Nichols locus (Oustaloup *et al.*, 1999a). This transfer function is used in section 3 for the construction of a network of iso-damping contours in the Nichols plane (Oustaloup *et al.*, 1995a).

Section 4 describes the CRONE (the French acronym of “Commande Robuste d’Ordre Non Entier”) control based on complex fractional order differentiation (Samko *et al.*, 1993; Miller *et al.*, 1993; Oustaloup and Mathieu, 1999b). This control methodology can be applied to SISO and MIMO plants and also plants with lightly damped modes. The interest of the fractional order is to define a transfer function with few parameters and thus to simplify design and optimization of the control system.

Section 5 presents an example of a multivariable flexible structure which is an aircraft wing model made of a free-clamped beam with a water tank and co-localized piezoelectric ceramics used as actuators to limit the vibrations and as sensors to measure these vibrations. The different levels of filling of the tank make it possible to test the robustness of the damping factor obtained with the CRONE control-design associated to iso-damping contours. In section 6, conclusions are given on the efficiency of fractional active control.

## 2. Complex fractional integration

The transfer function of a real fractional or non-integer integrator of order  $n$  is given by:

$$\beta(s) = \left( \frac{\omega_{cg}}{s} \right)^n, \quad n \in \mathbb{R}. \quad [1]$$

The Nichols locus of a transfer function described by this integrator in a frequency interval  $[\omega_A, \omega_B]$  is a vertical segment that will be called “vertical template” (Figure 1). The phase placement of this segment at the crossover frequency  $\omega_{cg}$  depends on the order  $n$  and is  $-n90^\circ$ .

From the extension of the description of the vertical template, the “generalized template” - that is to say an any-direction straight line segment in the Nichols plane - can be obtained using the complex non-integer integration of order  $n$ .  $n = a + ib$  where the imaginary unit  $i$  of the integration order  $n$  is independent of the imaginary unit  $j$  of the variable  $s$  ( $s = \sigma + j\omega$ ). The transfer function of a complex non-integer integrator of order  $n$  is given by:

$$\beta(s) = \left( \cosh\left(b \frac{\pi}{2}\right) \right)^{\text{sign}(b)} \left( \frac{\omega_{cg}}{s} \right)^a \left( \text{Re}_i \left[ \left( \frac{\omega_{cg}}{s} \right)^{ib} \right] \right)^{-\text{sign}(b)}. \quad [2]$$

The real part  $a$  defines the phase placement of the generalized template at  $\omega_{cg}$ ,  $-\text{Re}(n)90^\circ$ , and then the imaginary part  $b$  defines its angle to the vertical (Figure 1).

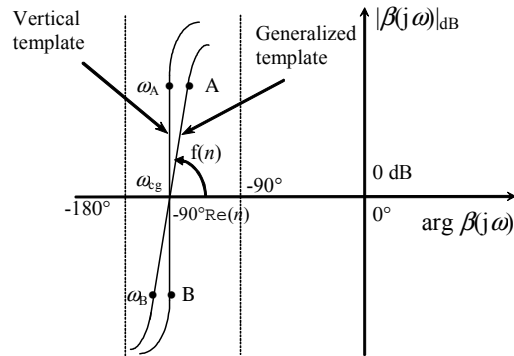


**Figure 1.** Representation of the vertical template and of the generalized template in the Nichols plane

### 3. Isodamping contours

In the time domain, the dynamic performance can be characterized by the first overshoot and the damping factor of a step response. In order to guarantee this performance by using a frequency domain control methodology, it is necessary to have an equivalent of this dynamic performance in the frequency domain. The well-known magnitude contour in the Nichols plane can be considered as an iso-overshoot contour (Oustaloup *et al.*, 2003). For the damping factor, Oustaloup *et al.* have constructed and defined a set of contours called “iso-damping” contours whose graduations are the damping factors in the Nichols plane (Oustaloup *et al.*, 1995a). These contours have been constructed using an envelope technique. The contour is then defined as the envelope tangented by a set of segments (Figure 2). In the Nichols plane, each segment of the set can be considered as the rectilinear part of an open-loop Nichols locus that ensures the closed-loop damping factor corresponding to the contour. This rectilinear part around gain crossover frequency,  $\omega_{t_g}$ , is the “generalized template” defined above.

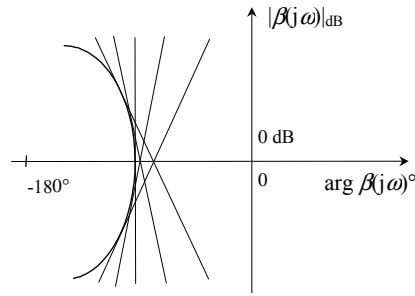


**Figure 2.** Envelope defining an isodamping contour in the Nichols plane

Isodamping contours can be defined analytically using a polynomial equation determined by interpolation of graphical data of each contour (Oustaloup *et al.*, 1995a). A contour  $\Gamma_\zeta$  is thus defined by:

$$\Gamma_\zeta = \left\{ M(X, Y) \in P, X - \sum_{j=0}^2 f_j(\zeta) Y^{2j} = 0 \right\} \quad [3]$$

with:

$$f_j(\zeta) = \sum_{k=0}^3 a_{jk} \zeta^k, \quad [4]$$

$X$  and  $Y$  being the coordinates expressed respectively in degrees and in decibels and  $a_{jk}$  the coefficients given in table 1.

**Table 1** - Values of coefficients  $a_{jk}$

$j/k$	0	1	2	3
0	-180.36	117.7	-74.316	40.376
1	-1.1538	3.8888	-5.2999	2.5417
2	-0.0057101	0.0080962	-0.0060354	0.0016158

#### 4. CRONE control

CRONE control system design (Oustaloup *et al.*, 1999; Oustaloup *et al.*, 2000) is a frequency-domain based methodology using complex fractional integration and the common unity feedback configuration. CRONE control is used for the robust control of perturbed linear plants. It consists on determining the nominal and optimal open-loop transfer function that guarantees the required specifications. This methodology uses fractional derivative orders (real or complex) as high level parameters that make easier the difficult design and optimization of the control-system, the plant perturbation being taken into account without any overestimation. Three Crone control generations have been developed, successively extending the application fields (Oustaloup *et al.*, 1995b; Pommier *et al.*, 2001). In this paper, the third generation will be, for the first time, applied to a lightly damped MIMO plant.

##### 4.1. Open-loop transfer function

The open-loop transfer function (Figure 3) of the initial third generation Crone method is based on the generalized template described previously and takes into account:

- the accuracy specifications at low frequencies,
- the generalized template around the frequency  $\omega_{tg}$ ,
- the plant behaviour at high frequencies in accordance with input sensitivity specifications for these frequencies.

For stable minimum-phase plants, this function is written:

$$\beta(s) = \beta_l(s)\beta_m(s)\beta_h(s) . \quad [5]$$

-  $\beta_m(s)$ , based on complex non-integer integration, is the transfer function describing the band-limited generalized template (Oustaloup *et al.*, 1999b; Oustaloup *et al.*, 2000):

$$\beta_m(s) = K \left( \frac{1 + \frac{s}{\omega_h}}{1 + \frac{s}{\omega_l}} \right)^a \left[ \operatorname{Re}_{i^i} \left\{ \left[ \frac{1 + \left( \frac{\omega_{cg}}{\omega_l} \right)^2}{1 + \left( \frac{\omega_{cg}}{\omega_h} \right)^2} \right]^{\frac{1}{2}} \left( \frac{1 + \frac{s}{\omega_h}}{1 + \frac{s}{\omega_l}} \right)^{ib'} \right\} \right]^{-q' \operatorname{sign}(b')} \quad [6]$$

$q'$  and  $b'$  being computed to avoid discontinuity of the phase (Pommier, 2002) and  $K$  being computed to ensure a gain of 0 dB at  $\omega_{cg}$ .

-  $\beta_l(s)$  is the transfer function of an order  $n_l$  proportional-integrator, whose corner frequency equals the low corner frequency of  $\beta_m(s)$ , so that joining  $\beta_l(s)$  and  $\beta_m(s)$  does not introduce extra parameters.  $\beta_l(s)$  is defined by:

$$\beta_l(s) = \left( 1 + \frac{\omega_l}{s} \right)^{n_l} \quad [7]$$

Integer order  $n_l$  is chosen such that the accuracy specification can be met.

-  $\beta_h(s)$  is the transfer function of order  $n_h$  low-pass filter, whose corner frequency equals the high corner frequency of  $\beta_m(s)$ , so that joining  $\beta_h(s)$  and  $\beta_m(s)$  does not introduce extra parameters.  $\beta_h(s)$  is defined by:

$$\beta_h(s) = 1 / \left( 1 + \frac{s}{\omega_h} \right)^{n_h} \quad [8]$$

If  $n_{ph}$  is the order of asymptotic behavior of the plant in high frequency ( $\omega \gg \omega_h$ ), order  $n_h$  is given by  $n_h \geq n_{ph}$ , with  $n_h = n_{ph}$  ensuring invariability of the input sensitivity function with the frequency and  $n_h > n_{ph}$  ensuring decrease.

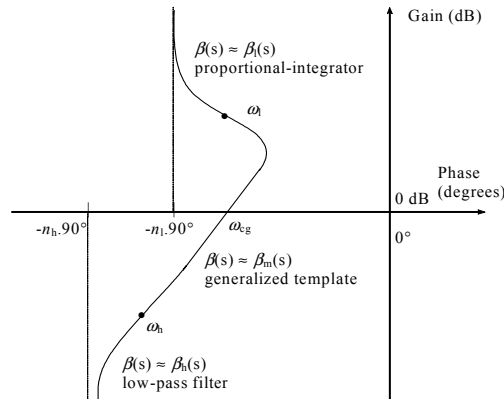


**Figure 3.** Different parts of the open-loop Nichols locus

#### 4.2. CRONE methodology for SISO plants

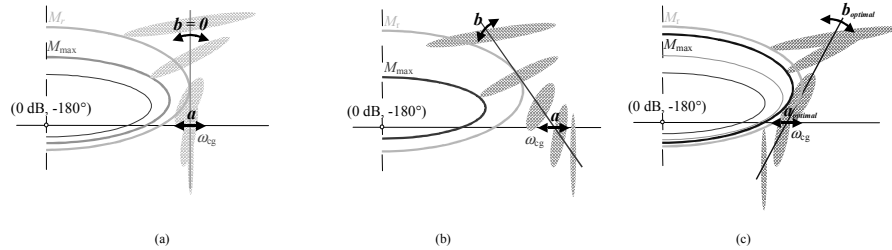


**Figure 4.** Optimal open-loop Nichols locus to position the uncertainty domains

The third generation CRONE methodology for SISO plants can be described in five points. The designer has:

1) to determine the nominal plant transfer function and the frequency uncertainty domains. For a given frequency, an uncertainty domain (called “template” by the QFT users (Horowitz, 1991)) is the smallest hull including the possible frequency responses of the plant. The use of the edge of the domains makes it possible to take into account the uncertainty with the smallest number of data. To construct this domain with a good probability to take into account all the possible plants even if the number of considered plants is limited, the simplest way is to define it convexly;

2) to specify some parameters of the open-loop transfer function defined for the nominal state of the plant: the gain cross-over frequency and the integer orders  $n_l$  and  $n_h$ ;

3) to specify bounds of the sensitivity functions;

4) to run a constrained nonlinear optimization that gives the parameters  $a$  and  $b$  and the frequencies  $\omega_l$  and  $\omega_h$  that correspond to the optimal open-loop Nichols locus. An open-loop Nichols locus is defined as optimal if it tangents the common  $M_{r_{nom}}$  magnitude contour and if it minimizes the variations of  $M_r$  for the other parametric states or if it tangents the common isodamping contour and if it minimizes the variations of the damping factor for the other parametric states. By minimizing the cost function  $J = (M_{r_{max}} - M_{r_{min}})^2$  where  $M_{r_{max}}$  and  $M_{r_{min}}$  are the maximal and minimal value of resonant peaks  $M_r$  or  $J = (\mathcal{E}_{max} - \mathcal{E}_{min})^2$  where  $\mathcal{E}_{max}$

and  $\mathcal{E}_{min}$  are the maximal and minimal value of the closed-loop damping factors  $\mathcal{E}$ , the optimal open-loop Nichols locus positions the uncertainty domains correctly, so that they overlap the low stability margin areas as little as possible (Figure 4: case (c)) is the best configuration). The minimization of  $J$  is carried out under a set of shaping constraints on the four usual sensitivity functions;

5) to compute the controller. While taking into account the plant right half-plane zeros and poles, the controller is deduced by the frequency-domain system

identification of the ratio of  $\beta_{\text{nom}}(j\omega)$  to the nominal plant function transfer  $G_{\text{nom}}(j\omega)$ . The resulting controller  $C(s)$  is a rational transfer function.

### 4.3. CRONE methodology for MIMO plants

#### 4.3.1. Principle

The CRONE methodology for  $n$  by  $n$  MIMO plants consists in finding a diagonal open-loop transfer matrix:

$$\beta_0 = \text{diag}[\beta_{0_i}] \quad [9]$$

whose  $n$  elements are fractional order transfer functions.

It is parametered to satisfy the four following objectives:

- perfect decoupling for the nominal plant,
- accuracy specifications at low frequencies,
- required nominal stability margins of the closed loops (behaviours around the required cut-off frequencies),
- specifications on the  $n$  control efforts at high frequencies.

After an optimization of the diagonal open-loop transfer matrix (relation [9]), the fractional controller matrix is computed from the relation [10] and synthesized by frequency-domain identification.

$$C(s) = G_0^{-1}(s)\beta_0(s) \quad [10]$$

#### 4.3.2. Optimized solution

Let  $G_0$  be the nominal plant transfer matrix such that  $G_0(s) = [g_{ij}(s)]_{i,j \in N}$  and let  $\beta_0$  be:

$$\beta_0 = G_0 C = \text{diag}[\beta_{0_i}] = \text{diag} \left[ \frac{n_i}{d_i} \right]_{i \in N} \quad [11]$$

where:

- $g_{ij}(s)$  is a strictly proper transfer function,
- $N = \{1, \dots, n\}$ ,
- $\beta_{0_i} = \frac{n_i}{d_i}$  is the element of the  $i^{\text{th}}$  column and row.



As mentioned above the aim of CRONE control for MIMO plants is to find a decoupling controller for the nominal plant.  $G_0$  being not diagonal, the problem is to find a decoupling and stabilizing controller  $C$  (Vardulakis, 1987). This controller exists if and only if the following hypotheses are true:

$$- H_1 : [G_0(s)]^{-1} \text{ exist ,} \quad [12]$$

$$- H_2 : Z_+[G_0(s)] \cap P_+[G_0(s)] = 0 , \quad [13]$$

where  $Z_+[G_0(s)]$  and  $P_+[G_0(s)]$  indicate the positive real part zero and pole sets.

The controller  $C(s)$  is:

$$C = G_0^{-1} \beta_0 = \frac{\text{adj}(G_0)}{|G_0|} \text{diag} \left[ \frac{n_i}{d_i} \right]_{i \in N} \quad [14]$$

with  $\text{adj}(G_0(s)) = [G_0^{ij}(s)]^T = [G_0^{ji}(s)]$ ,  $G_0^{ij}(s)$  being the cofactor corresponding to element  $g_{ij}(s)$  and  $|G_0|$  corresponding to determinant of  $G_0(s)$ .

Thus each term of the matrix  $C$  is:

$$c_{ij} = \frac{G_0^{ji}}{|G_0|} \beta_{0_i} \quad \forall i, j \in N \quad [15]$$

The nominal sensitivity and the complementary sensitivity transfer function matrices are:

$$S_0(s) = [I + \beta_0(s)]^{-1} = \text{diag}[S_{0_i}(s)]_{1 \leq i \leq n} \quad [16]$$

$$T_0(s) = [I + \beta_0(s)]^{-1} \beta_0(s) = \text{diag}[T_{0_i}(s)]_{1 \leq i \leq n} \quad [17]$$

with:

$$T_{0_i}(s) = \frac{\beta_{0_i}(s)}{(1 + \beta_{0_i}(s))} \quad [18]$$

$$S_{0_i}(s) = \frac{1}{(1 + \beta_{0_i}(s))} \quad [19]$$

For plants other than the nominal, the closed-loop transfer matrices  $T(s)$  and  $S(s)$  are no longer diagonal. Each diagonal element  $T_{ii}(s)$  and  $S_{ii}(s)$  could be interpreted as closed-loop transfer functions coming from a scalar open-loop transfer function  $\beta_{ii}(s)$  called equivalent open-loop transfer function:

$$\beta_{ii}(s) = \frac{T_{ii}(s)}{1 - T_{ii}(s)} = \frac{1 - S_{ii}(s)}{S_{ii}(s)} \quad [20]$$

For each nominal open-loop  $\beta_0(s)$ , many generalized templates can border the same required contour in the Nichols plane. The optimal one minimizes the robustness cost function:

$$J = \sum_{i=1}^n (M_{r_{\max_i}} - M_{r_{\min_i}})^2 \quad \text{or} \quad J = \sum_{i=1}^n (\varepsilon_{\max_i} - \varepsilon_{\min_i})^2 \quad [21]$$

where  $M_r$  is the resonant peak and  $\varepsilon$  the damping factor, while respecting the following set of inequalities for  $\omega \in \mathbb{R}$  and  $i, j \in N$ :

$$\inf_G |T_{ij}(j\omega)| \geq T_{ij_l}(\omega) \quad [22]$$

$$\sup_G |T_{ij}(j\omega)| \leq T_{ij_u}(\omega) \quad [23]$$

$$\sup_G |S_{ij}(j\omega)| \leq S_{ij_u}(\omega) \quad [24]$$

$$\sup_G |CS_{ij}(j\omega)| \leq CS_{ij_u}(\omega) \quad [25]$$

$$\sup_G |SG_{ij}(j\omega)| \leq SG_{ij_u}(\omega) \quad [26]$$

where  $G$  is the set of all perturbed plants.

As the uncertainties are taken into account by the least conservative method, a non-linear optimization method must be used to find the optimal values of the independent parameters of the fractional open-loop transfer function.

#### 4.4. Extension to resonant plants

Let  $G_0$  be the nominal plant transfer matrix such that  $G_0(s) = [g_{ij}(s)]_{i,j \in N}$  with  $g_{ij}(s) = g_{0_{ij}}(s) \cdot h_{ij}(s)$  and  $h_{ij}(s)$  the transfer including the resonant modes of the plant.

Let  $P_0$  be the inverse of  $G_0$  such that  $P_0(s) = [p_{ij}(s)]_{i,j \in N}$  with  $p_{ij}(s) = p_{0_{ij}}(s) \cdot m_{ij}(s)$  and  $m_{ij}(s)$  the transfer including the resonant modes of the inverse of the plants.

The aim of this section is to show that the resonant modes of the plant and of the inverse of the plant must be included in the open-loop transfer function  $\beta_0$  to ensure that all closed-loop transfer functions are damped enough (Nelson Gruel *et al.*, 2007).

The first transfer matrix to be considered is the input-disturbance sensitivity,  $T_0 C^{-1}$ . Using:

$$T_0 C^{-1} = S_0 G_0 = \left[ \frac{d_i(s) \cdot g_{0_{ij}}(s) \cdot h_{ij}(s)}{d_i(s) + n_i(s)} \right] \quad [27]$$

this transfer function is resonant-free if:

$$d_i(s) = \frac{\hat{d}_i(s)}{h_{ij}(s)} \quad \forall j \in N \quad [28]$$

that is to say if  $d_i(s)$  contains the resonant modes  $h_{ij}(s)$ ,  $\hat{d}_i(s)$  being then the part of the denominator  $d_i(s)$  without the resonant modes .

The denominator of the  $i^{\text{th}}$  open-loop transfer function must satisfy all the following equations:

$$d_i(s) = \frac{\hat{d}_i(s)}{h_{i1}(s)}, d_i(s) = \frac{\hat{d}_i(s)}{h_{i2}(s)}, \dots, d_i(s) = \frac{\hat{d}_i(s)}{h_{in}(s)} \quad [29]$$

and therefore:

$$d_i(s) = \frac{\hat{d}_i(s)}{H_i(s)} \quad \forall i \in N \quad [30]$$

where the transfer functions  $H_i(s)$  have in common the lightly damped modes of the  $i^{\text{th}}$  row of  $G_0$ .

The second transfer matrix to be considered is input sensitivity  $C S$ . Using:

$$C_0 S = G_0^{-1} T = \left[ \frac{p_{0_{ij}}(s) \cdot m_{ij}(s) \cdot n_j(s)}{d_j(s) + n_j(s)} \right] \quad [31]$$

this transfer function is resonant-free if:

$$n_j(s) = \frac{\hat{n}_j(s)}{m_{ij}(s)} \quad \forall i \in N \quad [32]$$

that is to say if  $n_j(s)$  contains the resonant modes  $m_{ij}(s)$ ,  $\hat{n}_j(s)$  being then the part of the numerator  $n_j(s)$  without the resonant modes .

The numerator of the  $i^{\text{th}}$  open-loop transfer function must satisfy all the following equations:

$$n_j(s) = \frac{\hat{n}_j(s)}{m_{1j}(s)}, n_j(s) = \frac{\hat{n}_j(s)}{m_{2j}(s)}, \dots, n_j(s) = \frac{\hat{n}_j(s)}{m_{nj}(s)} \quad [33]$$

and therefore:

$$n_j(s) = \frac{\hat{n}_j(s)}{M_j(s)} \quad \forall j \in N \quad [34]$$

where the transfer functions  $M_j(s)$  have in common some lightly damped modes of the  $j^{\text{th}}$  column of  $G_0^{-1}$ .

Adding some lightly damped modes on the open-loop transfer functions causes resonant frequencies to appear on sensitivity and complementary sensitivity transfer functions. To attenuate their effect, notch or peak transfer function  $Q_j(s)$  is included in  $\beta_0(s)$  around each resonant frequency such that:

$$Q_j(s) = \left( \left( \frac{s}{\omega_j} \right)^2 + 2\varepsilon \frac{s}{\omega_j} + 1 \right) / \left( \left( \frac{s}{\omega'_j} \right)^2 + 2\varepsilon' \frac{s}{\omega'_j} + 1 \right) \quad [35]$$

where  $\omega_j$  and  $\omega'_j$  are frequencies close to the resonant frequency and  $\varepsilon$  and  $\varepsilon'$  are the damping factors.

## 5. Robust control of a lightly damped plant with isodamping property

### 5.1. Description of the plant

The plant under study is an aircraft wing model (see figure 5). It is made of a beam and a tank. This structure has the same resonant frequencies as a real air wing. The problem is to control the vibrations which depend on the levels of filling of the tank. Two sets of piezoelectric ceramics, bonded at the clamp of the beam, are used as actuators to fight against bending and twisting vibrations. Two others piezoelectric ceramics, co-localised with the actuators, are used as sensors to measure the vibrations.

The characteristics of the plant are given in table 2.

**Table 2.** Plant characteristics

	Beam	Actuator x 2		Tank
<i>Length (mm)</i>	1360	140	<i>Ext. Diameter (mm)</i>	110
<i>Width (mm)</i>	160	75	<i>Int. Diameter (mm)</i>	105
<i>Thickness (mm)</i>	5	0.5	<i>Length (mm)</i>	700
<i>Density (kg/m<sup>3</sup>)</i>	2970	7800	<i>x-location (mm)</i>	1280
<i>Young Modulus (Gpa)</i>	75	67	<i>Plastic Density (kg/m3)</i>	1180
<i>Piezoelectric Const. (pm/V)</i>	-	-210	<i>Young Modulus (Gpa)</i>	4.5

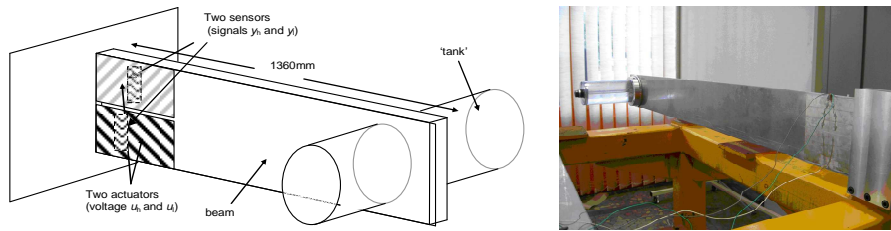


**Figure 5.** Model of the structure (beam with the tank)

## 5.2. Modelling and identification of the plant

### 5.2.2. MIMO Model

The plant is described by a 2x2 MIMO model. The two inputs are the two actuators voltages (called  $u_1$  and  $u_h$ ) and the two outputs are the sensors voltages (called  $y_1$  and  $y_h$ ). The plant is described by the matrix of transfer functions given by:

$$G(s) = \begin{bmatrix} G_{11}(s) & G_{12}(s) \\ G_{21}(s) & G_{22}(s) \end{bmatrix} \quad [36]$$

and the transfer functions will be identified thanks to the relation:

$$\begin{bmatrix} y_h \\ y_1 \end{bmatrix} = G(s) \begin{bmatrix} u_h \\ u_1 \end{bmatrix} \quad [37]$$

A preliminary study using finite elements has shown that it is necessary to take into account the first three modes of resonance of the aircraft wing model. These modes are the first two modes of flexion and the first mode of twisting which are too close to allow neglecting one of them. The representation of the deformations of the first three modes can be used to establish the form of the model and in particular the contribution of each mode in each transfer function. If you note:

- $F_{1ij}(s)$  the transfer function of the first mode of flexion relative to the actuator  $i$  and the sensor  $j$ ,
- $F_{2ij}(s)$  the transfer function of the second mode of flexion relative to the actuator  $i$  and the sensor  $j$ ,
- $T_{1ij}(s)$  the transfer function of the first mode of bending relative to the actuator  $i$  and the sensor  $j$ ,
- $R_{ij}$  the static term relative to the actuator  $i$  and the sensor  $j$  (Rubin, 1975),

the [2x2] matrix of the aircraft wing model that takes into account the first three modes is written :

$$G(s) = \begin{bmatrix} G_{11}(s) & G_{12}(s) \\ G_{21}(s) & G_{22}(s) \end{bmatrix} = \begin{bmatrix} F1_{11} + F2_{11} + T1_{11} + R1_{11} & F1_{12} + F2_{12} - T1_{12} + R1_{12} \\ F1_{21} + F2_{21} - T1_{21} + R1_{21} & F1_{22} + F2_{22} + T1_{22} + R1_{22} \end{bmatrix} \quad [38]$$

As sensors and actuators are co-localised, the contributions of each mode are summed for the diagonal terms and the contribution of the twisting mode is subtracted for the non diagonal terms.

### 5.2.3. Model identification

Measurements are necessary to establish the model since the finite elements analysis has made it possible to determine the modes of resonance of the model but not the values of the damping coefficients. The four transfer functions are identified so that their Bode diagrams correspond to the measures. They are all of the form:

$$G_{ij}(s) = \frac{k_{ij1}}{\frac{s^2}{\omega_{ij1}^2} + 2 \frac{\epsilon_{ij1} s}{\omega_{ij1}} + 1} + \frac{k_{ij2}}{\frac{s^2}{\omega_{ij2}^2} + 2 \frac{\epsilon_{ij2} s}{\omega_{ij2}} + 1} + \frac{k_{ij3}}{\frac{s^2}{\omega_{ij3}^2} + 2 \frac{\epsilon_{ij3} s}{\omega_{ij3}} + 1} + R_{ij} \quad [39]$$

with  $i$  and  $j$  between 1 and 2 and the numerical data of the tables 6 to 9 .

**Table 3.** Values for  $G_{11}(s)$

		Empty tank	Half-full tank	Full tank
1° mode of flexion	$k_{111}$	0,015	0,006	0,01
	$\omega_{111}$ (rad/s)	7,22	5,1	4,59
	$\epsilon_{111}$	0,0061	0,0062	0,0045
2° mode of flexion	$k_{112}$	0,01	0,002	0,005
	$\omega_{112}$ (rad/s)	53,78	41,2	34,84
	$\epsilon_{112}$	0,012	0,046	0,006
1° mode of twisting	$k_{113}$	0,01	0,005	0,001
	$\omega_{113}$ (rad/s)	134,5	96,6	21,6
	$\epsilon_{113}$	0,012	0,01	0,015
static term	$R_{11}$	0,12	0,14	0,085

The figure 6 gives the Bode diagrams of these four transfer functions and shows that the model is very lightly damped and uncertain because of the variations of the filling of the tank. The curves with the lower frequency resonance correspond to the full tank and the curves with the higher frequency resonance correspond to the empty tank.

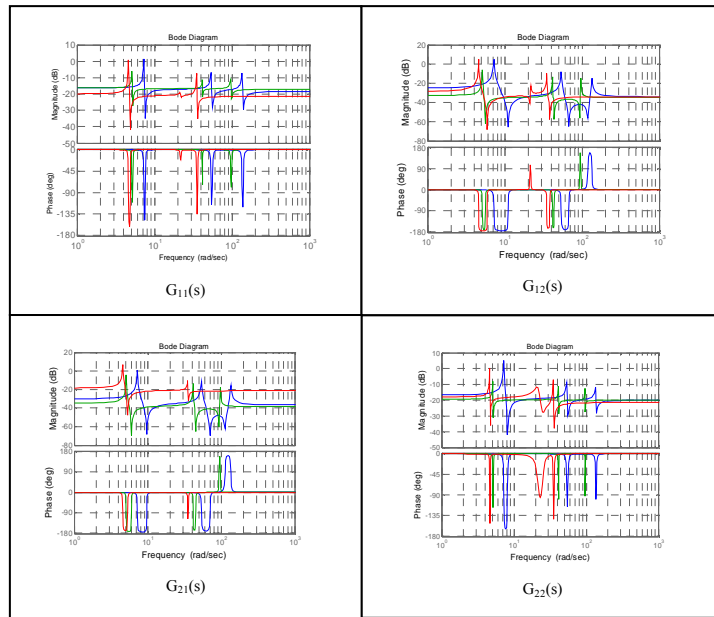


Figure 6. Bode diagrams of the four terms of the plant matrix

Table 4. Values for  $G_{12}(s)$

		Empty tank	Half-full tank	Full tank
1° mode of flexion	$k_{121}$	0,032	0,004	0,015
	$\omega_{121}$ (rad/s)	7,22	5,1	4,59
	$\epsilon_{121}$	0,0087	0,0039	0,0041
2° mode of flexion	$k_{122}$	0,008	0,002	0,004
	$\omega_{122}$ (rad/s)	53,78	41,2	34,84
	$\epsilon_{122}$	0,01	0,0046	0,006
1° mode of twisting	$k_{123}$	-0,004	-0,0012	-0,001
	$\omega_{123}$ (rad/s)	134,5	96,6	21,6
	$\epsilon_{123}$	0,011	0,0032	0,007
static term	$R_{12}$	0,02	0,018	0,02

**Table 5.** Values for  $G_{21}(s)$ 

		Empty tank	Half-full tank	Full tank
<b>1° mode of flexion</b>	$k_{211}$	0,014	0,005	0,03
	$\omega_{211}$ (rad/s)	7,22	5,1	4,59
	$\epsilon_{211}$	0,0061	0,0039	0,0068
<b>2° mode of flexion</b>	$k_{212}$	0,0065	0,002	0,004
	$\omega_{212}$ (rad/s)	53,78	41,2	34,84
	$\epsilon_{212}$	0,012	0,0046	0,0069
<b>1° mode of twisting</b>	$k_{213}$	-0,004	-0,001	0
	$\omega_{213}$ (rad/s)	134,5	96,6	21,6
	$\epsilon_{213}$	0,012	0,0039	x
<b>static term</b>	$R_{21}$	0,015	0,012	0,085

**Table 6.** Values for  $G_{22}(s)$ 

		Empty tank	Half-full tank	Full tank
<b>1° mode of flexion</b>	$k_{221}$	0,02	0,004	0,007
	$\omega_{221}$ (rad/s)	7,22	5,1	4,59
	$\epsilon_{221}$	0,0087	0,0052	0,0034
<b>2° mode of flexion</b>	$k_{222}$	0,009	0,0022	0,005
	$\omega_{222}$ (rad/s)	53,78	41,2	34,84
	$\epsilon_{222}$	0,0129	0,0046	0,0056
<b>1° mode of twisting</b>	$k_{223}$	0,006	0,0011	0,03
	$\omega_{223}$ (rad/s)	134,5	96,6	21,6
	$\epsilon_{223}$	0,0126	0,0026	0,067
<b>static term</b>	$R_{22}$	0,1	0,1	0,085

### 5.3. CRONE control

The plant being a 2x2 MIMO system, the open-loop transfer function matrix is written as:

$$\beta(s) = \begin{bmatrix} \beta_{01}(s) & 0 \\ 0 & \beta_{02}(s) \end{bmatrix} \quad [40]$$

whose two diagonal terms are defined by CRONE open-loop transfer functions of third generation (equ. [8]).

The nominal plant corresponds to the empty tank. The objectives are to increase the damping factor of the closed-loop system to get a value of 0.1 after control, whatever the filling of the tank. So the iso-damping contour that each open-loop transfer function should tangent is of value 0.1. For each of the open-loop transfer function, the following configuration has been chosen:

- gain cross-over frequency equal to 3 rad/s,
- order  $n_l = -1$  in order to limit the gain of the controllers at low frequency and order  $n_h = 4$  in order to limit the amplification of the noise at high frequency,



- minimum of the complementary sensibility function  $T$  equal to -5dB (for the frequencies below the gain-cross over frequency) to bound the controller effect at low frequency,
- maximum of the function  $CS$  equal to 50dB to bound the controller amplitude at high frequency,
- maximum of the sensibility function  $S$  equal to 20dB to bound the controller effect at high frequency.

This configuration has also been chosen in order to get - after optimization – the terms of the matrix of the controller with a high gain on a large band of frequencies so that the control of vibrations is efficient and in order to position the uncertainties domains so that they do not penetrate the performance contour.

Let's now take into account the lightly damped modes of the plant. There are no lightly damped modes on the rows of the plant matrix but there are three lightly damped modes in the columns of the inverse matrix of the plant coming from the determinant of the matrix since:

$$[G_0(s)]^{-1} = \frac{\text{adj}(G_0)}{\det(G_0)} \quad [41]$$

Therefore, it is necessary to introduce in the open-loop transfer functions  $\beta_{01}(s)$  and  $\beta_{02}(s)$  the resonances of the modes at 7,09 rad/s, 8,12 rad/s and 57,11 rad/s.

Finally, a filter has been added in the open-loop transfer functions. It aims at shaping the open-loop Nichols locus by decreasing the gain and increasing the phase locally around the first resonance so that the uncertainties domains do not overlap the contours. The expression of the filter is the same for the two open-loop transfer functions and is written:

$$\beta_r(s) = \left( \frac{s^e}{7^2} + 0.2 \frac{s}{7} + 1 \right) / \left( \frac{s^e}{9^2} + 2 \frac{s}{9} + 1 \right) \quad [42]$$

Results have been obtained thanks to a constrained nonlinear optimization. Initial values of parameters are well-chosen to avoid the stabilization of the optimization on bad local minima. The results of the optimization lead to the following optimal parameters:

- for  $\beta_{01}(s)$ :  $a=0.0037$ ,  $b^*=3.05$  ;  $q^*=5$  ;  $\omega_1=1.4$  rad/s ;  $\omega_2=3.3$  rad/s ;  $Y_t = 0.4$ dB (open-loop gain for the tangency point between the contour and the open-loop Nichols locus),

- for  $\beta_{02}(s)$ :  $a=2.99$ ,  $b^*=1.81$  ;  $q^*=5$  ;  $\omega_1=1.3$  rad/s ;  $\omega_2=3.3$  rad/s ;  $Y_t = 0.71$ dB.

The Nichols loci with the uncertainty domains are given in the Figure 7 for the two open-loop transfer functions  $\beta_{01}(s)$  and  $\beta_{02}(s)$ .

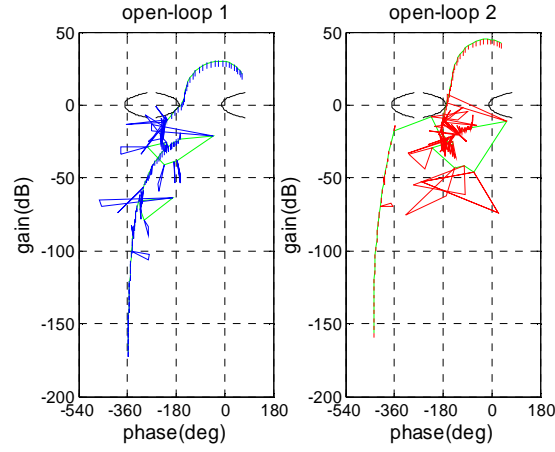


**Figure 7.** Nichols loci for  $\beta_{01}(s)$  and  $\beta_{02}(s)$

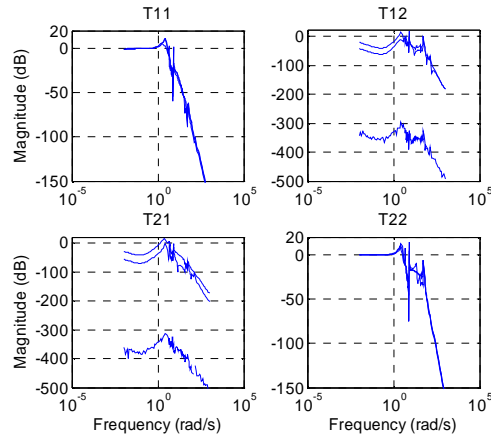


**Figure 8.** Bode diagrams of the terms of the complementary sensibility functions matrix

The Figure 8 gives the four terms of the complementary sensibility functions matrix. It shows that the matrix is diagonal for the nominal state and that the controller is thus decoupling. It also shows that the closed-loop transfer functions are less resonant than the plant transfer functions.

The matrix of the controller is computed from the relation:

$$C(s) = G_0^{-1}(s)\beta(s) = \begin{bmatrix} C_{11}(s) & C_{12}(s) \\ C_{21}(s) & C_{22}(s) \end{bmatrix} \quad [43]$$

The four terms of this matrix are synthesized by identification in the frequency domain and the Bode diagrams are given in the Figure 9.

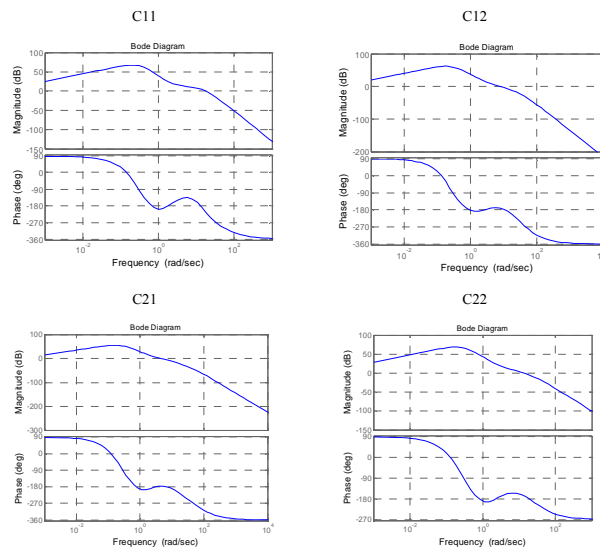


**Figure 9.** Bode diagrams of the terms of the controller matrix

#### 5.4. Results

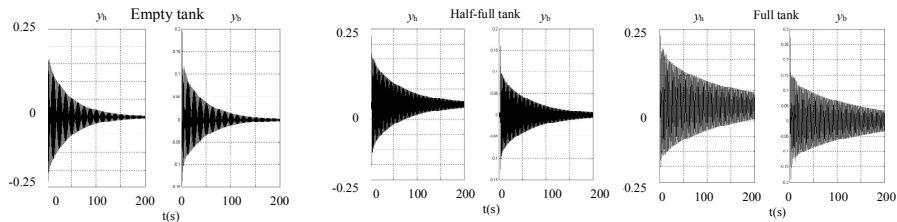


**Figure 10.** Response to a disturbance without control

The figure 9 shows the free response to a disturbance (the wing model is pushed back from its equilibrium with a movement of flexion and of twisting and then released) in three cases (empty tank, half-full tank and full tank). This disturbance could be interpreted as an air bump for a real aircraft wing. Several tests have been achieved but the figure 10 only shows the results for one test. The figure gives the signal from the two sensors. It shows that it takes more than 200s to go back to balance.

The Figure 11 shows the response to the same disturbance as previously with the CRONE controller. This figure gives the signal from the two sensors and the voltage of the two actuators. Several observations can be drawn from this figure:

1) the voltages of the actuators are on their maximum level, even in saturation for the first oscillations since the D-Space card will limit the values of  $u_h$  and  $u_b$  at 1V (which corresponds to 130V on the actuator).

2) it takes now less than 25s to go back to balance.

3) the CRONE controller guarantees the robustness of the damping factor of the response. The Table 7 gives the value of this ratio for the three cases and the two sensors.

**Table 7.** Values of the damping factor for the 3 configurations of the tank with the CRONE controller

	Sensor $y_h$	Sensor $y_b$
Empty tank	0,11	0,11
Half-full tank	0,1	0,1
Full tank	0,12	0,12

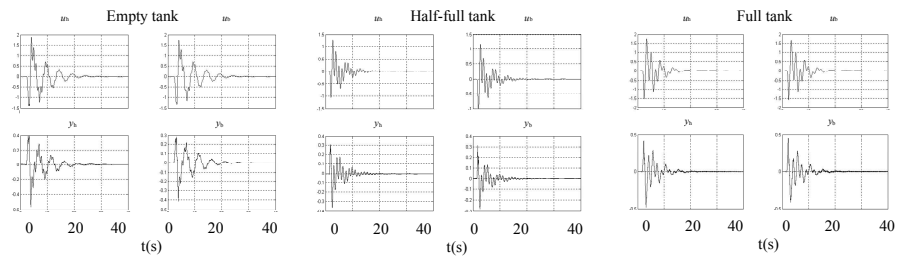


**Figure 11.** Response to a disturbance with the CRONE control

## 6. Conclusion

This article presents fractional robust control with isodamping property. The plant under study is an aircraft wing model with a water tank. It is a multivariable plant with lighted damped modes. The proposed methodology is CRONE control. Results show that the vibrations are better damped with the CRONE control and that the time to go back to balance is divided by a factor 10. The tests on the plant with various levels of filling of the tank made it possible to highlight the properties of robustness of the damping factor. The use of multivariable CRONE methodology and of isodamping contours to carry out the control of a flexible structure with isodamping property is thus clearly relevant.

## 7. References

- Horowitz I.M., "Quantitative feedback design theory – QFT", *QFT Publications*, Boulder, Colorado, 1991.
- Miller K.S., Ross B., "An introduction to the fractional calculus and fractional differential equations", *John Wiley & Sons Inc.*, New York, 1993.
- Nelson Gruel D., Lanusse P., Oustaloup A., Pommier V., "Robust control system design for multivariable plants with lightly damped modes", *ASME conference, IDETC/CIE*, Las Vegas, USA, Sept. 4-7, 2007.
- Oustaloup A., Mathieu B., Lanusse P., « Intégration non entière complexe et contours d'isoamortissement », *APII*. vol. 29, n° 2, 1995a.
- Oustaloup A., Mathieu B., Lanusse P., "The CRONE control of resonant plants: application to a flexible transmission", *European Journal of Control*, vol. 1, p. 113-121, 1995b.
- Oustaloup A., Sabatier J. and Lanusse P., "From fractal robustness to the CRONE Control", *Fractional Calculus and Applied Analysis*, An international Journal for Theory and Applications, vol. 2, p. 1-30, 1999a.
- Oustaloup A., Mathieu B., « La commande CRONE : du scalaire au multivariable », Editions Hermès, Paris, 1999b.
- Oustaloup A., Melchior P., Lanusse P., Cois O., Dancla F., "The CRONE toolbox for Matlab", *11th IEEE International Symp. on Computer-Aided Control System Design, CACSD*, Anchorage, Alaska, USA, September 25-27, 2000.
- Oustaloup A., Pommier V., Lanusse P., "Design of a fractional control using performance contours. Application to an electromechanical system", *Fractional Calculus and Applied Analysis*, vol. 6, n° 1, 2003.
- Pommier V., Lanusse P., Sabatier J., Oustaloup A., "Input-output linearization and fractional robust control of a non linear system", *European Control Conference ECC01*, 4-7 Septembre, Porto, Portugal, 2001.
- Pommier V., Commande non entière et commande robuste non linéaire d'un banc d'essais hydraulique, Thèse de l'Ecole nationale des Arts et Métiers, 2002.
- Rubin S., "Improved component-mode representation for structural dynamic analysis", *AIAA Journal*, vol. 13, n° 8, 1975, p. 995-1006.
- Samko S.G., Kilbas A.A., Marichev O.I., "Fractional integrals and derivatives", *Gordon and Breach Science Publishers*, 1993.
- Vardulakis A. I. G., "Internal stabilization and decoupling in linear multivariable systems by unity output feedback compensation", *IEEE Trans. on Autom. Control*, 32, August, 1987.
- Yq C., Moore K.L., "Relay feedback tuning of robust PID controllers with isodamping property", *IEEE Trans. on systems, Man and Cybernetics*, partB-Cybernetics 35 (1), Feb, 2005, p23-31.